Sub-lethal toxicity of five disinfection by-products on microalgae determined by flow cytometry – Lines of evidence for adverse outcome pathways

Théo Ciccia, Pascal Pandard, Philippe Ciffroy, Nastassia Urien, Léo Lafay, Anne Bado-Nilles

Ecotoxicology and Environmental Safety 266 (2023) 115582

Contents lists available at ScienceDirect

Ecotoxicology and Environmental Safety

journal homepage: www.elsevier.com/locate/ecoenv

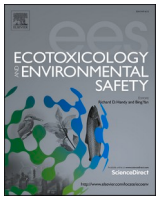

Sub-lethal toxicity of five disinfection by-products on microalgae determined by flow cytometry – Lines of evidence for adverse outcome pathways

Théo Ciccia [a,*], Pascal Pandard [b], Philippe Ciffroy [a], Nastassia Urien [a], Léo Lafay [a], Anne Bado-Nilles [b]

[a] Laboratoire National d'Hydraulique et Environnement (LNHE), Division Recherche et Développement, Electricité de France (EDF), 6 Quai de Watier, 78401 Chatou Cedex 01, France
[b] Institut National de l'Environnement Industriel et des Risques (INERIS), Parc Technologique Alata, BP 2, 60550 Verneuil-en-Halatte, France

ARTICLE INFO

Edited by G Liu

Keywords:
Disinfection by-products
Microalgae
Growth inhibition
Flow cytometry
Biomarkers

ABSTRACT

Standardised tests are often used to determine the ecotoxicity of chemicals and focus mainly on one or a few generic endpoints (e.g. mortality, growth), but information on the sub-cellular processes leading to these effects remain usually partial or missing. Flow cytometry (FCM) can be a practical tool to study the physiological responses of individual cells (such as microalgae) exposed to a stress via the use of fluorochromes and their morphology and natural autofluorescence. This work aimed to assess the effects of five chlorine-based disinfection by-products (DBPs) taken individually on growth and sub-cellular endpoints of the green microalgae *Raphidocelis subcapitata*. These five DBPs, characteristic of a chlorinated effluent, are the following monochloroacetic acid (MCAA), dichloroacetic acid (DCAA), trichloroacetic acid (TCAA), bromochloroacetic acid (BCAA) and 1,1-dichloropropan-2-one (1,1-DCP). Results showed that 1,1-DCP had the strongest effect on growth inhibition ($EC_{50} = 1.8$ mg.L^{-1}), followed by MCAA, TCAA, BCAA and DCAA (EC_{50} of 10.1, 15.7, 27.3 and 64.5 mg.L^{-1} respectively). Neutral lipid content, reactive oxygen species (ROS) formation, red autofluorescence, green autofluorescence, size and intracellular complexity were significantly affected by the exposure to the five DBPs. Only mitochondrial membrane potential did not show any variation. Important cellular damages (>10%) were observed for only two of the chemicals (BCAA and 1,1-DCP) and were probably due to ROS formation. The most sensitive and informative sub-lethal parameter studied was metabolic activity (esterase activity), for which three types of response were observed. Combining all this information, an adverse outcome pathways framework was proposed to explain the effect of the targeted chemicals on *R. subcapitata*. Based on these results, both FCM sub-cellular analysis and conventional endpoint of algal toxicity were found to be complementary approaches.

1. Introduction

Among the diversity of aquatic organisms, unicellular algae are commonly used in ecotoxicology. Microalgae bioassays were some of the first established and standardised for determining phytotoxic effects of chemicals, wastewater and environmental samples (Lewis, 1990). Their ubiquity in aquatic environments, their role as primary producers (production of biomass and oxygen and prey for higher trophic levels), their short life cycle and their sensitivity to a wide variety of substances have made them a group of organisms of interest in ecotoxicity testing (Nyholm and Källqvist, 1989; Silva et al., 2009). That way, any kind of disturbance observed on the algal population in the environment could affect the entire ecosystem. The unicellular freshwater alga *Raphidocelis subcapitata* is one of the most commonly used microalgae in ecotoxicology, and more precisely in the chronic OECD test guideline no. 201 (Ceschin et al., 2021) because of its high growth rate and short generation time (Rojíčková and Maršálek, 1999; Yamagishi et al., 2017).

Originally, ecotoxicity assays on microalgae were mainly focused on the increase of cellular density, with growth rate as the final endpoint. Although ecologically relevant, this endpoint only represents a response at the population level and does not allow the identification of potential modes of action (MoAs) and mechanistic effects at sub-cellular levels.

* Corresponding author.
E-mail address: theo.ciccia@edf.fr (T. Ciccia).

https://doi.org/10.1016/j.ecoenv.2023.115582
Received 26 May 2023; Received in revised form 6 October 2023; Accepted 11 October 2023
Available online 20 October 2023

Knowledge of the MoA at sub-cellular levels is of great interest, for example to establish adverse outcomes pathways (AOPs) of targeted molecules, or to predict combined effects in the case of co-exposure to chemical mixtures thanks to models of joint action (Ankley et al., 2010; Faust et al., 2003). Recent developments in flow cytometry (FCM) techniques make it possible to observe morphological and/or physiological effects of stressors on individual algal cells (Čertnerová and Galbraith, 2021). Indeed, light scattering parameters (size and cell complexity) and autofluorescence parameters (natural pigment content) can be measured directly by FCM for each cell (Adan et al., 2017). Furthermore, the use of fluorescent probes allows to study physiological responses of individual cells exposed to a stress, such as the formation of reactive oxygen species (ROS), cell viability, metabolic activity or changes in neutral lipid content (Almeida et al., 2019; Franklin et al., 2001; Machado and Soares, 2021). Consequently, it is possible to combine the conventional endpoint based on algal growth inhibition (OECD, 2011) with morphological and physiological measurements, providing early responses to chemical exposure and a better understanding of toxic mechanisms/modes of action. In particular, the FCM techniques have been used to study the sub-cellular effects of chemical substances on algal cells, especially on the *R. subcapitata* species, whether for metals, antibiotics or pesticides (Almeida et al., 2021; Franklin et al., 2001; Machado and Soares, 2015, 2019). However, most ecotoxicological studies only investigate a single exposure time and generally not the sensitivity of early physiological responses after chemical exposure. Moreover, the same studies mainly focus on cellular viability, metabolic activity and oxidative stress, and parameters such as neutral lipid content (carbon and energy storage), mitochondrial membrane potential (mitochondrial bioenergetic state) and green autofluorescence have often been ignored (GAF).

Chlorine-based disinfectants are widely used for drinking water secondary disinfection but also as biocidal treatment in some industrial cooling systems, to prevent the development of pathogenic microorganisms in cooling water systems (Coniglio et al., 2015; Dupuy et al., 2011). After use in cooling systems, chlorinated waters are released to the environment and residual chlorine-based disinfectants may be discharged into receiving waters. In natural waters, free chlorine, and to a lesser extent monochloramine, act as oxidants and react with natural organic matter (NOM) (Ciffroy and Urien, 2021; Dong et al., 2021; Duirk et al., 2005, 2002). NOM oxidation by chlorine-based disinfectants is particularly important because it results in disinfection by-products (DBPs) formation, mainly trihalomethanes (THMs), haloacetic acids (HAAs), haloacetonitriles (HANs) and haloketones (HKs) (Cowman and Singer, 1996; Diehl et al., 2000; Vikesland, 2001; Richardson and Postigo, 2011). About 800 DBPs have been identified so far, but more than 50% of total DBPs are still unknown (Dong et al., 2021). Although chlorine-based disinfectants are intended to specifically target pathogens, their by-products were shown to exhibit toxicity towards aquatic organisms, whether algae (Cui et al., 2022, 2021; Roberts et al., 2010), macrophytes (Hanson and Solomon, 2004), invertebrates (Labine and Simpson, 2021) or fish (Fisher et al., 2014; Hanigan et al., 2017).

In light of this background, the objective of this paper was to (i) assess the sensitivity of sub-lethal parameters and their changes over time with FCM analyses, (ii) assess the toxicity of 5 DBPs of concern on the unicellular green algae *R. subcapitata* and (iii) identify their MoAs, helping us gain a better understanding of the underlying mechanisms leading to growth inhibition. Monochloroacetic acid, dichloroacetic acid, trichloroacetic acid, bromochloroacetic acid and 1,1-dichloropropan-2-one, are considered to be the typical and main DBPs formed during the disinfectant treatment of French nuclear power plants (internal data, not published). Their individual effects on esterase activity, cellular viability, mitochondrial membrane potential, oxidative stress, lipid content, red autofluorescence (RAF), green autofluorescence (GAF), size, complexity and cellular density of microalgal cells exposed for 72 h, were assessed in the exposure conditions of the algal growth inhibition test.

2. Materiel and methods

2.1. Chemicals

The disinfection by-products monochloroacetic acid (MCAA; purity 99 + %) and trichloroacetic acid (TCAA; purity 99 + %) were purchased from Thermo Scientific™. Bromochloroacetic acid (BCAA; purity 97%) was purchased from Sigma-Aldrich. Dichloroacetic acid (DCAA; purity 99 + %) was purchased from Alfa Aesar. Haloketone 1,1-dichloropropan-2-one (1,1-DCP), also known as 1,1-dichloroacetone (purity 95%), was purchased from Novachemistry. CAS numbers are detailed in Table S1. Stock solutions were prepared directly in the OECD TG 201 growth medium.

2.2. Chemical analyses

To quantify DBPs concentrations to which algae were exposed, analyses in the test medium were carried out by sampling three out of seven concentrations for every HAA (one low, one middle and one high concentration) and six out of seven for 1,1-DCP at the beginning and at the end of each assay (the latter being less stable than HAAs). Measurements were made by liquid-liquid extraction-gas chromatography-mass spectrometry (LLE-GC-MS). During the 72 h tests, all the HAAs were found to be stable in the OECD medium except for the 1,1-DCP for which important loss was observed for each exposure condition. Therefore, the exposure concentrations were calculated using the time-weighted mean method. The concentrations for which the chemical analyses were not performed were corrected using the linear regression equation drawn at each time (0 and 72 h) based on the measured chemical concentrations.

2.3. Microalgae cultures

The freshwater microalgae *Raphidocelis subcapitata* (previously known as *Pseudokirchneriella subcapitata*) was used for all the tests. The strain was purchased from Culture Collection of Algae and Protozoa (CCAP 278/4; Dunbeg, UK). The stock culture used in this study was maintained in 250 mL glass flasks containing 100 mL Lefevre-Czarda medium at 23 ± 2 °C, on an orbital shaker (100–150 rpm) and with a dark:light cycle of 8:16 h, and renewed once a week. Pre-cultures were inoculated (0.6–1 mL of stock culture) in 100 mL OECD 201 medium (OECD, 2011) for 96 h in 250 mL Erlenmeyer flasks on an orbital shaker (125 rpm), in a temperature range between 21.3 and 23.3 °C and under continuous light condition (60–120 $\mu E.m^{-2}.s^{-1}$). These conditions and exposure duration ensured that algae were in exponential growth phase when used to launch the inhibition tests. Microalgal cultures, pre-cultures, and experimental media were systematically manipulated in sterile environment. Algal cell concentrations used for growth-rate determination were measured with a Coulter counter (Beckman Coulter Z2, Villepinte, France).

2.4. Exposure of R. subcapitata to the disinfection by-products

Growth inhibition tests were conducted according to the OECD 201 guideline (OECD, 2011). In each individual test, cells were exposed for 72 h in Erlenmeyer glass flasks filled with a total volume of 100 mL of OECD 201 medium and seven different concentrations of one DBP (see Table S1 in supplementary material) previously determined based on preliminary range-finding tests. After determination of cellular density of the pre-cultures (exponentially growing algal cells) with a haemocytometer, an initial concentration of 10^4 $cell.mL^{-1}$ was inoculated in each test vessel. No renewal was carried out during the 72-h test. Incubation conditions for light exposure, shaking and temperature were identical to the ones described above for pre-cultures. Three replicates with algae and one replicate without algae (negative control) were carried out for each concentration. For the control condition (algae

without treatment), six replicates were prepared. Flasks were sampled at 24, 48 and 72 h for flow cytometry analysis, and at 72 h for coulter. Density measurements were made on the coulter because preliminary tests highlighted important loss during cell counting with the FCM compared to the Coulter counter.

Based on the measurements made at 72 h with the Coulter counter, algal growth rate was determined for each test concentration using the following equation:

$$\mu_{i-j} = (\ln(X_j) - \ln(X_i))/(t_j - t_i)\,(day^{-1}) \quad (1)$$

where $\mu_{i\text{-}j}$ is the average specific growth rate from time i to j, X_i is the cell density at time i and X_j the cell density at time j.

2.5. Flow cytometry (FCM) measurements of morphological and physiological endpoints

Samples at 24, 48 and 72 h were collected for each cellular parameter analysis, placed in a 96-well plate (300 µL per well, without cellular concentration standardisation), and analyses were performed using a MACSQuant X flow cytometer (Miltenyi Biotec, Bergisch Gladbach, Germany). The 488 nm excitation laser was used for all the measured parameters, and B1-H (525–550 nm) and B3-H (655–730 nm) emission detectors were used for data collection. An acquisition threshold corresponding to the lowest possible size for the algal cells was set with FSC-H channel and used for all analyses, allowing us to remove unwanted particles (cellular or medium debris for example). The maximum number of measured events was set at 10 000 for each sample and the data used for most of the cellular parameters was the median intensity fluorescence (MFI) value, except for esterase activity and cellular viability expressed as a percentage of marked cells, and ROS formation with the use of the mean intensity fluorescence (Fig. S1).

The conditions of fluorochrome incubation were determined prior to this study by running optimization experiments for each fluorochrome, taking into account concentration, time, temperature and light conditions. Aliquots of fluorochrome stock solutions were prepared in dimethyl sulfoxide (DMSO) and stored at − 18 °C until use. Working solutions were then made in the medium with a final concentration of DMSO < 0.01%. During the experiments, two concentrations of copper (II) sulfate ($CuSO_4$) were tested (0.08 and 0.12 $mg.L^{-1}$) to be used as positive control for the FCM measurements based on preliminary tests. Furthermore, negative controls were used to check if any external contamination happened during the experiment and if the fluorochromes reacted with the medium without the presence of algae.

2.5.1. Cell size, complexity, and natural pigments content

Cell size and intracellular complexity were measured by displaying respectively side (SSC-A) and forward (FSC-A) light scatter versus cell count. The intracellular complexity measured by flow cytometry provides information on intracellular granularity (density of internal structures) of the cell (Adan et al., 2017). Red autofluorescence (RAF), corresponding to chlorophyll *a* fluorescence and the photochemical activity of Photosystem II (PS II), was estimated using the B3-H channel only at 72 h (Franklin et al., 2001). Green autofluorescence (GAF) (Cheloni and Slaveykova, 2018; Kleinegris et al., 2010) was estimated using the B1-H channel.

2.5.2. Cellular viability

To discriminate between viable and non-viable cells, the fluorescence of cells stained with propidium iodide (PI; ThermoFisher Invitrogen™) was measured and incubation was adapted from Seoane et al. (2017b). This specific fluorochrome is only able to enter a cell with damaged cell membranes and intercalates with double stranded nucleic acids to produce red fluorescence collected in the B3-H channel. Samples were incubated with propidium iodide for 20 min in the dark at room temperature on a plate shaker (600 rpm) and at a concentration of 7.3 µM. Cell viability was expressed as a percentage of non-viable cells located in a gated zone present on the cytogram.

2.5.3. Mitochondrial membrane potential

Mitochondrial membrane potential (ΔΨm) was assessed using Rhodamine 123 (Rho123; ThermoFisher Invitrogen™) and adapted from Liu et al. (2008). This cell-permeant fluorochrome accumulates in mitochondria. Inhibition of ATP synthase on exposed cells leads to an increase of ΔΨm which stops Rho123 from being transported outside of mitochondria and results in an increase in fluorescence intensity (Chae et al., 2016; Machado et al., 2015). This gives information on the status of mitochondrial function, and therefore the capacity of the cell to produce energy. The green fluorescence emission of this compound was collected in the B1-H channel. During the experiments, samples were incubated with Rho123 for 120 min in the dark, at room temperature, on a plate shaker (600 rpm) at a concentration of 12.9 µM. Mitochondrial membrane potential was expressed as the median fluorescence intensity (MFI) value of marked cells for each sample.

2.5.4. Reactive oxygen species (ROS) formation

The fluorochrome 2′,7′-dichlorodihydrofluorescein diacetate (H_2DCFDA; ThermoFisher Invitrogen™) was used to monitor the changes in non-specific ROS formation inside the cells and incubation conditions were adapted from Dupraz et al. (2019). After diffusing passively in the cell, H_2DCFDA is hydrolysed by esterase to form the non-fluorescent 2′,7′-dichlorodihydrofluorescein (H_2DCF), which is then converted to the highly fluorescent 2′,7′-dichlorofluorescein (DCF) when oxidised in the presence of ROS. Samples were incubated with H_2DCFDA for 30 min in the dark at room temperature, on a plate shaker (600 rpm) and at a concentration of 0.3 µM. B1-H detector was used to measure the fluorescence emitted by DCF. Mean fluorescence intensity value was used to express ROS formation (with subtraction of mean GAF intensity) for each sample instead of median fluorescence intensity because of GAF interference occurring at the same wavelength range. Additional data were extracted on size and complexity to dissociate mono- and multinucleated cells. Grouping of mono- and multinucleated cells in gated zones was done arbitrarily based on visual observations made on the cytograms for the different experiments (Fig. S1-F2).

2.5.5. Neutral lipid content

The lipophilic fluorochrome 4,4-difluoro-1,3,5,7-tetramethyl-4-bora-3a,4a-diaza-*s*-indacene (Bodipy$^{505/515}$; ThermoFisher Invitrogen™) was used to determine the intracellular neutral lipid content, primarly triacylglycerol (TAG) which accumulates in the form of lipid droplets and serves as storage of carbon and energy in microalgae (Hu et al., 2008). The incubation conditions were adapted from Steadman Tyler et al. (2019). Collected samples were incubated with Bodipy$^{505/515}$ for 90 min in the dark at room temperature and on a plate shaker (600 rpm) and at a concentration of 19.8 µM. Lipid content was expressed as the median fluorescence intensity (MFI) value of marked cells for each sample.

2.5.6. Esterase activity

Esterase activity was determined using fluorescein diacetate (FDA; ThermoFisher Invitrogen™) and adapted from Dupraz et al. (2019). The lipophilic non-fluorescent fluorochrome is diffused inside the cell by means of its acetoxymethyl group which is then hydrolysed (cleaved) by nonspecific esterase, dissociating fluorescein from the rest if the compounds. This molecule, excited by the laser at 488 nm, emits fluorescence observed on the B1-H emission detector. Samples were incubated with FDA for 30 min in the dark at room temperature, on a plate shaker (600 rpm). For this fluorochrome, concentrations were inoculated according to the cell density of each sample, ranging from 187.6 µM to 12×10^3 µM corresponding to cellular concentrations from under 1.6×10^4 $cell.mL^{-1}$ to 10^6 $cell.mL^{-1}$ (with a factor of two between each FDA concentration). Esterase activity was expressed as a percentage of

cell considered metabolically inactive (located in a gated zone called FDA- on the left of the cytogram), active (located in a gated zone called FDA+ in the middle of the cytogram) and stimulated (located in a gated zone called FDA++ on the right of the cytogram) (Figure F1-H). For each of these gates, additional data were extracted on size and complexity, to dissociate mono- and multinucleated cells.

2.6. Statistical analyses

Concentration-response curves used to determine the growth inhibition range of each experiment were modelled using R software (version 1.4.1717) with the *rjags* package and a R script version of $MOSAIC_{growth}$ (Charles et al., 2018). The script was run for each chemical and their 7 concentrations with the three-parameter log-logistic regression model (LL.3) under a Bayesian framework with the following equation:

$$Y = d \Big/ \left(1 + \left(\frac{x}{e}\right)^{b}\right) \quad (2)$$

where Y is the growth rate (μ, h^{-1}) corresponding to the concentration x and at 72 h, d is the upper-limit corresponding to the response value of controls, b is the slope of the curve and e is the concentration corresponding to the median effective concentration EC_{50}.

The cytometry data for each sub-lethal parameter are presented in the Results and Supplementary material with standard deviation (SD) and statistical significance. Statistical analyses were carried out between controls and exposed algal cells for each substance, and at each time step by one-way ANOVA, followed by Tukey-Kramer multiple comparison method. In the case of invalid test assumptions (not normally distributed data and/or non-homogeneous variance across groups), a non-parametric Kruskal-Wallis test was used followed by the multiple comparison Dunn's test.

3. Results

3.1. Growth rate inhibition

In this study, concentration-response curves of the algal growth were established for each chemical at 72 h and EC_{50}, EC_{10}, NOEC (no observed effect concentration) and LOEC (lowest observed effect concentration) were then determined and summarised in Table S2. Based on the EC_{50}, 1,1-DCP inhibited the most algal growth, followed by MCAA≥TCAA>BCAA>DCAA. The number of chlorine (Cl) and bromine (Br) did not seem to influence the toxicity of the five DBPs towards algae as no correlation was found between the structure and the toxicity of the chemicals.

3.2. Effects of DBPs on morphological and physiological endpoints over time

Data obtained for each cellular parameter and each DBP are presented in Figs. 1–7 and Figs. S2-S6. For clarity, these data are summarised in Table S3 by presenting LOEC and NOEC for each parameter and DBP with trends of increase or decrease compared to the control.

3.2.1. Effects of DBPs on cell size, intracellular complexity, and natural pigment content (GAF and RAF)

Data related to cell size and intracellular complexity are presented in Fig. 1 and Figs. S2-S3. Only cells exposed to MCAA for size and TCAA for both size and intracellular complexity showed significant changes ($p < 0.05$) at the earliest time of measure (24 h). At 48 h, size and complexity were significantly greater for microalgae exposed to all the DBPs ($p < 0.05$) except for DCAA. Finally, a significant increase in cellular size and complexity ($p < 0.05$) was observed at 72 h for the highest concentrations tested except for BCAA for which only the complexity was significantly higher. Over time, size and intracellular complexity peaked at 24 h and showed a slight decrease at 48 h and 72 h for all conditions including controls. Only microalgae exposed to 3.6 and 4.7 $mg.L^{-1}$ of 1,1-DCP, kept increasing in size and complexity at 48 h and 72 h ($p < 0.05$). Results also showed that both morphological parameters were well correlated, the increase of one being linked to the increase of the other (R^2=0.82, 0.78, 0.92, 0.92 and 0.89 for MCAA, DCAA, TCAA, BCAA and 1,1-DCP respectively) (Fig. S3).

Concerning GAF (Fig. 2), fluorescence increased significantly at the end of the experiments, i.e. at 72 h for the highest concentrations ($p < 0.05$). In the case of 1,1-DCP and DCAA, the increase was already significant at 48 h, and after 24 h for TCAA and BCAA. Over time, microalgae exposed to the highest concentrations of the five DBPs showed a decrease in GAF between 24 h and 48 h and an increase after 48 h leading to a peak of intensity at 72 h. At low and intermediate

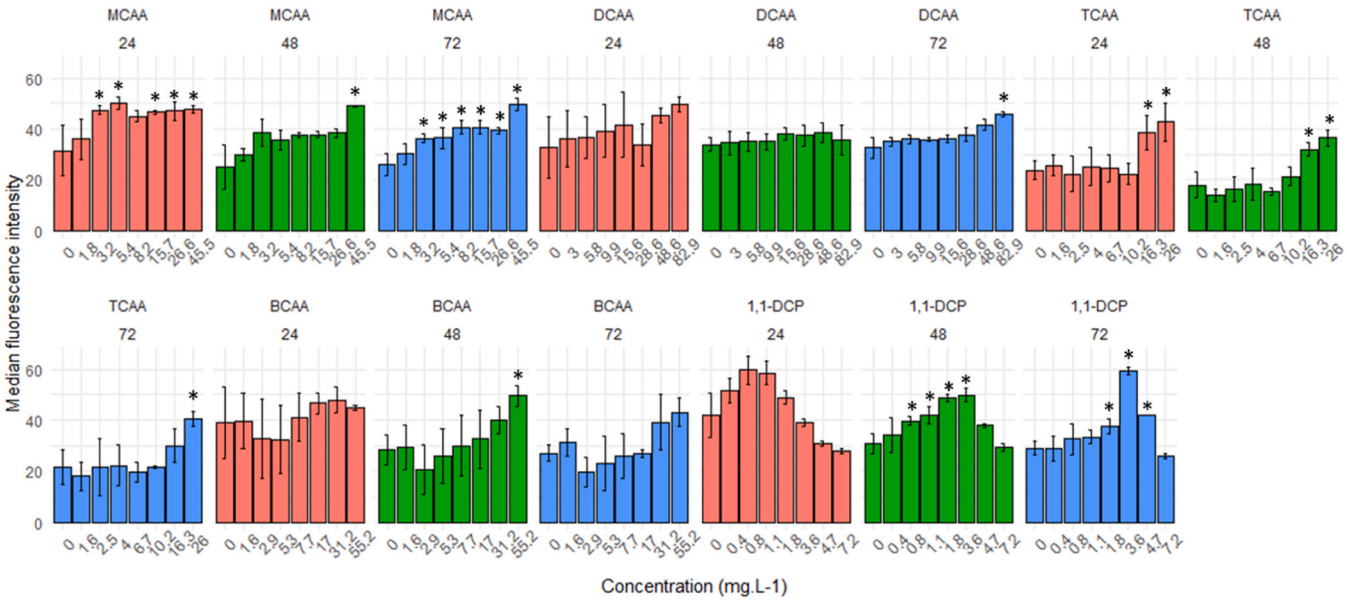

Fig. 1. *R. subcapitata* cell size (arbitrary unit) measured by flow cytometry for the five DBPs. *denote significant differences between treatment and control ($p < 0.05$).

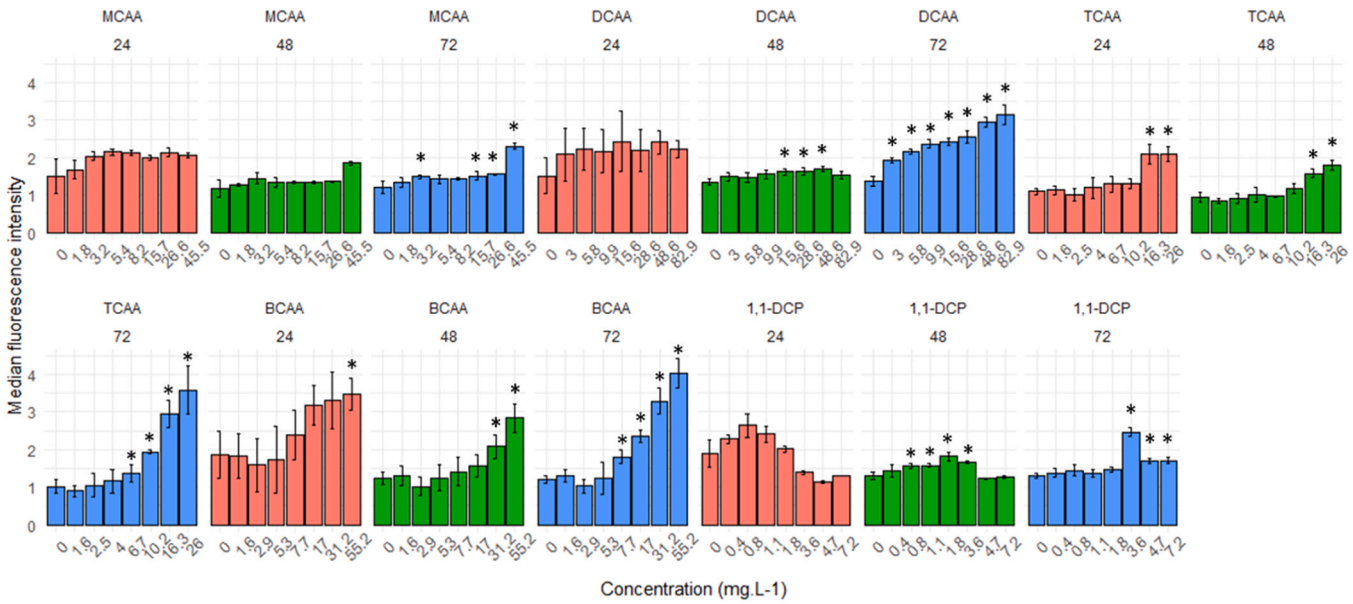

Fig. 2. *R. subcapitata* green autofluorescence (GAF - median fluorescence intensity, arbitrary unit) measured by flow cytometry for the five DBPs. *denote significant differences between treatment and control ($p < 0.05$).

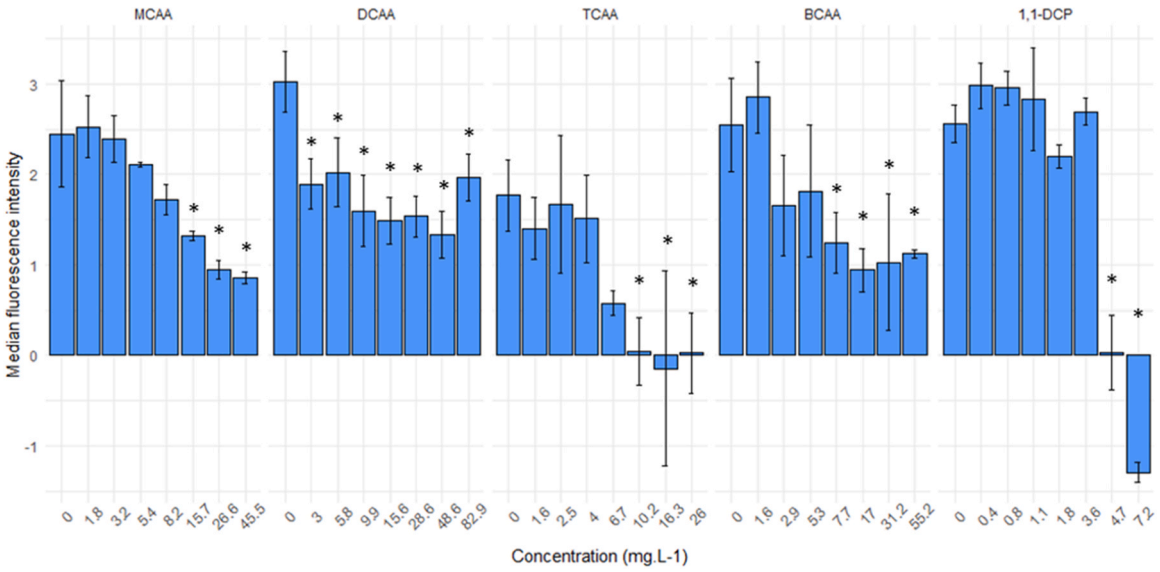

Fig. 3. *R. subcapitata* red autofluorescence (median fluorescence intensity, arbitrary unit) measured by flow cytometry for the five DBPs at 72 h. *denote significant differences between treatment and control ($p < 0.05$).

concentrations, the temporal trends were comparable to the controls with a low decrease observed between 24 h and 48 h followed by a stable fluorescence until 72 h.

Microalgae RAF (Fig. 3) was also studied at 72 h, and is considered to be representative of the chlorophyll *a* fluorescence and the photochemical activity of PS II (Almeida et al., 2019; Reynolds, 1984). Results showed that the exposure to all the single DBPs provoked a significant decrease in chlorophyll *a* fluorescence at 72 h ($p < 0.05$).

3.2.2. *Effects of DBPs on cell viability*

Data related to cell viability are presented in Fig. S4. They showed no significant changes after exposure to MCAA and TCAA at any point in time and concentration compared to controls ($p > 0.05$) (Table S3). Exposure to DCAA led to a significant decrease in non-viable cells at 48.6–82.9 mg.L^{-1} at 24 h (from 3.7% to 0.6%) and a significant increase at 82.9 mg.L^{-1} at 72 h (up to 5.9%, with 1.8% for control) ($p < 0.05$), but changes observed in both cases stayed in the low percentage range. An increasing trend was observed for BCAA at 48 h for the highest concentration (55.2 mg.L^{-1}) (15% of non-viable cells with high variability between replicates, 0.4% for control), with a similar result occurring at 72 h (10% of non-viable cells, 0.5% for control, but significant in this case ($p < 0.05$). Lastly, 1,1-DCP induced no significant effect at 24 h but mortality of the cells reached 26% at 0.8 mg.L^{-1} (with 8% for control, with high variability between replicates). A significant increase in non-viable cells was observed after exposure at 0.4–1.8 mg.L^{-1} at 48 h (up to 23%, with 2% for control) and at 0.4–3.8 mg.L^{-1} at 72 h (up to 7%, with 1% for control).

3.2.3. *Effects of DBPs on mitochondrial membrane potential (ΔΨm)*

Data related to mitochondrial membrane potential are presented in Fig. S5. In our study, use of Rho123 did not give any conclusive results. In fact, only the highest concentration (82.9 mg.L^{-1}) of DCAA exposure

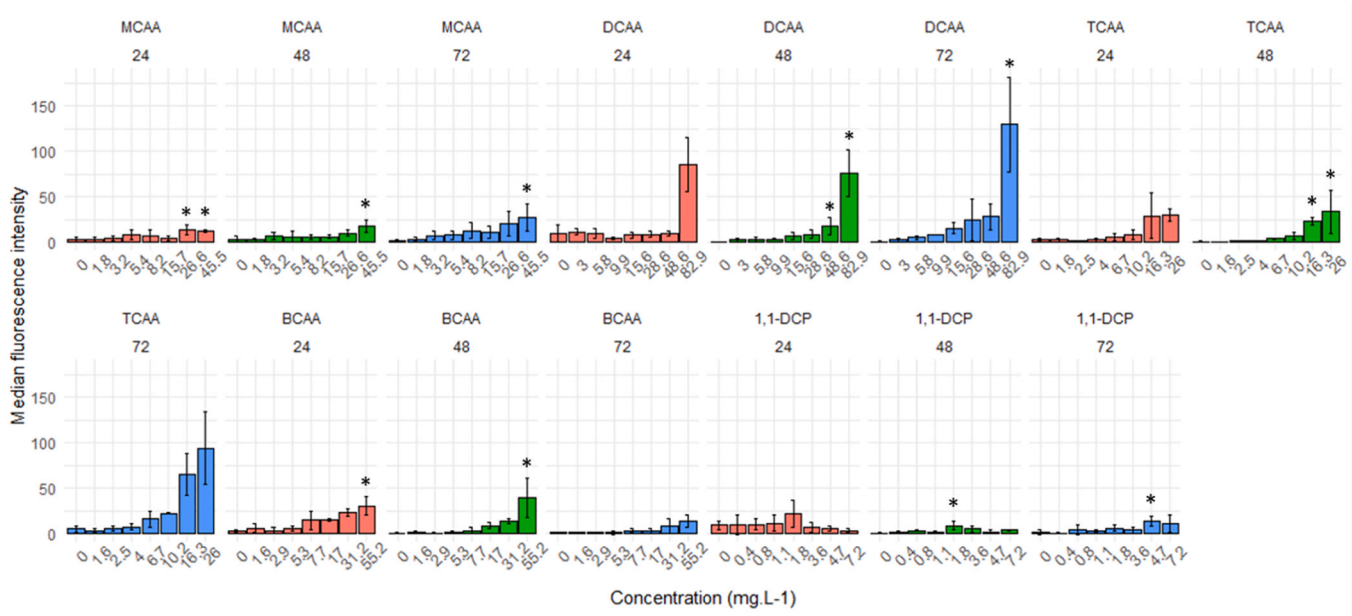

Fig. 4. ROS formation (mean fluorescence intensity, arbitrary unit) measured by flow cytometry for the five DBPs. *denote significant differences between treatment and control ($p < 0.05$).

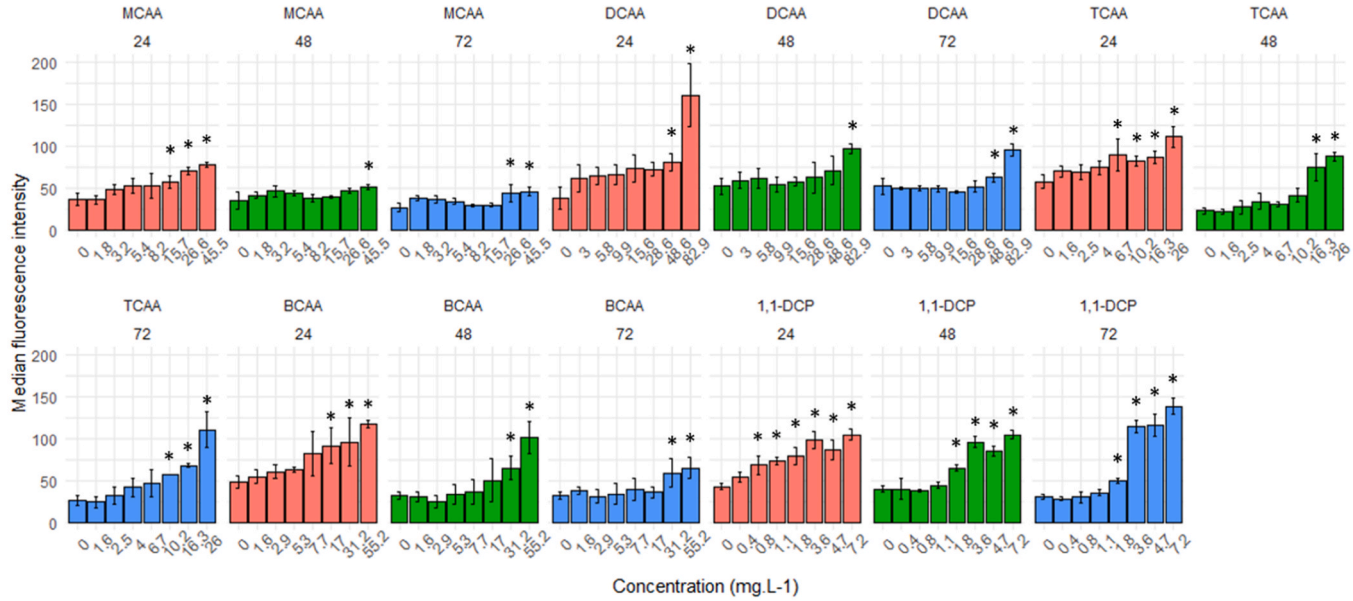

Fig. 5. Neutral lipid content (median fluorescence intensity, arbitrary unit) measured by flow cytometry for the five DBPs. *denote significant differences between treatment and control ($p < 0.05$).

showed a significant decrease ($p < 0.05$) in Rho123 fluorescence intensity at 48 h and 72 h compared to the control, which could be explained either by a potential inhibition of mitochondrial electron transport chain or damage to cell membrane resulting in the leak of the dye. For the rest of the DBPs, no significant changes were noticed at any time step and concentration. Over time, ΔΨm remained either stable (for TCAA and BCAA) or slightly decreased at 48 and/or 72 h ($p < 0.05$) (for MCAA and DCAA) for all conditions of exposure. Only for the three highest concentrations of 1,1-DCP, an increase was observed at the end of the experiment ($p < 0.05$).

3.2.4. *Effects of DBPs on ROS formation*

Data related to ROS formation are presented in Fig. 4. H_2DCFDA allowed us to observe the intracellular changes in ROS formation of *R. subcapitata*. Each DBP induced significant ROS formation at some concentrations and times. Significant effects ($p < 0.05$) were noticed at 24 h for MCAA for the highest concentrations tested and remained at 48 and 72 h. Significant increases in H_2DCFDA fluorescence intensity were also measured for the other HAAs at the highest exposure concentration but only at specific time point and not continuously (48 and 72 h for DCAA, 48 h for TCAA, 24 and48h for BCAA) ($p < 0.05$). However, the non-significant data still showed a systematic upward trend with the concentrations at every point in time. For 1,1-DCP, a significant increase was observed both at 48 h and 72 h for one intermediate concentration, 1.8 $mg.L^{-1}$ and 4.7 $mg.L^{-1}$ respectively ($p < 0.05$). Over time, controls and specific range of concentrations for three of the substances (all conditions for BCAA, 0–5.8 $mg.L^{-1}$ for DCAA and 0–3.6 $mg.L^{-1}$ for 1,1-DCP) showed a decreasing temporal trend either at 48 h or 72 h, or at

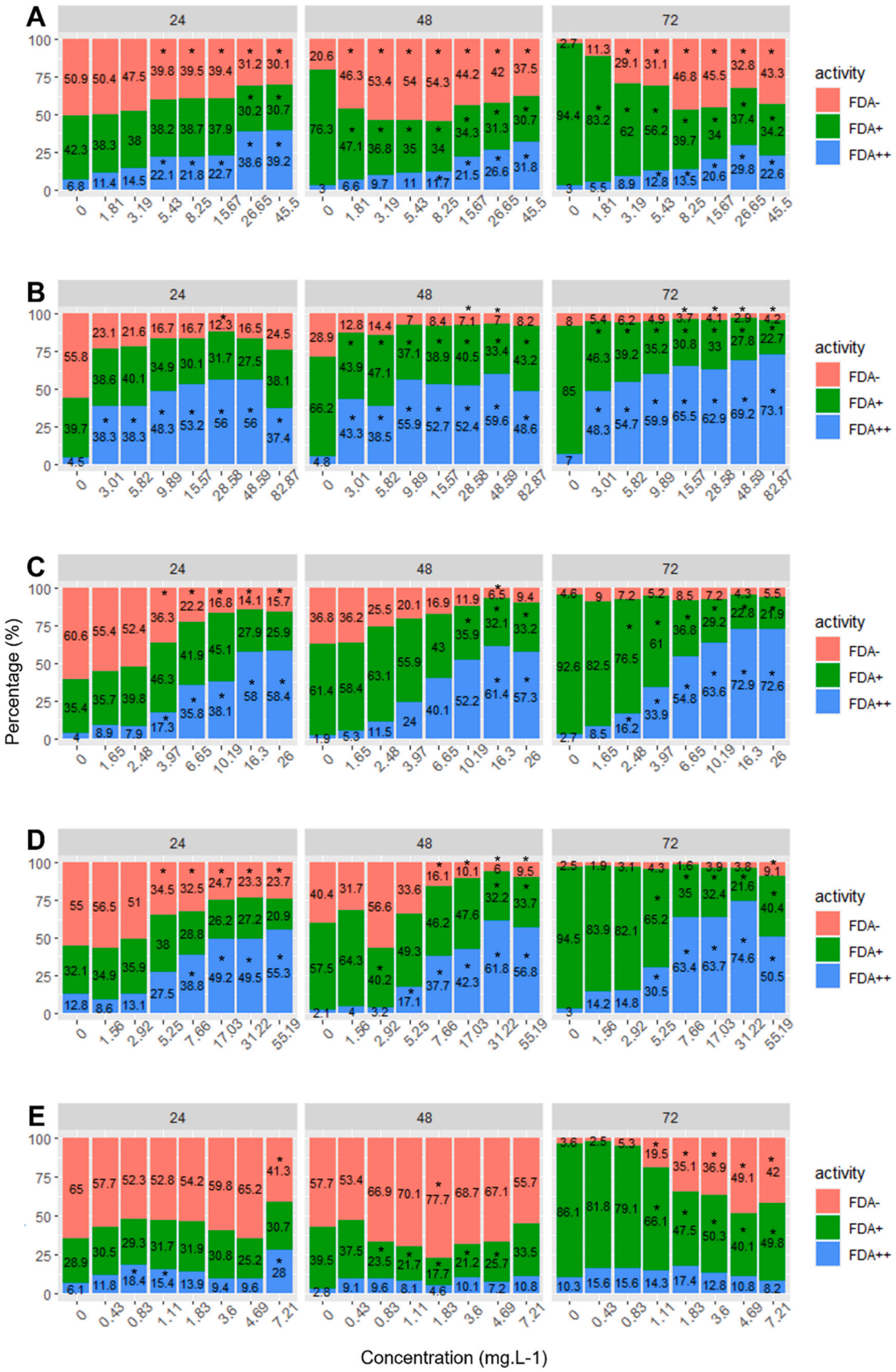

Fig. 6. Metabolic activity after exposure to the 5 DBPs individually (A=MCAA, B=DCAA, C=TCAA, D=BCAA and E = 1,1-DCP) is presented in this stacked plot, for each time and concentration. Data shown corresponds to the mean percentage of R. subcapitata in 3 different metabolic states (FDA- corresponding to a low/inactive metabolic activity, FDA+ to a normal metabolic activity and FDA++ to a stimulated metabolic activity) for each exposure condition. *denote significant differences between treatment and control ($p < 0.05$) for each respective metabolic activity.

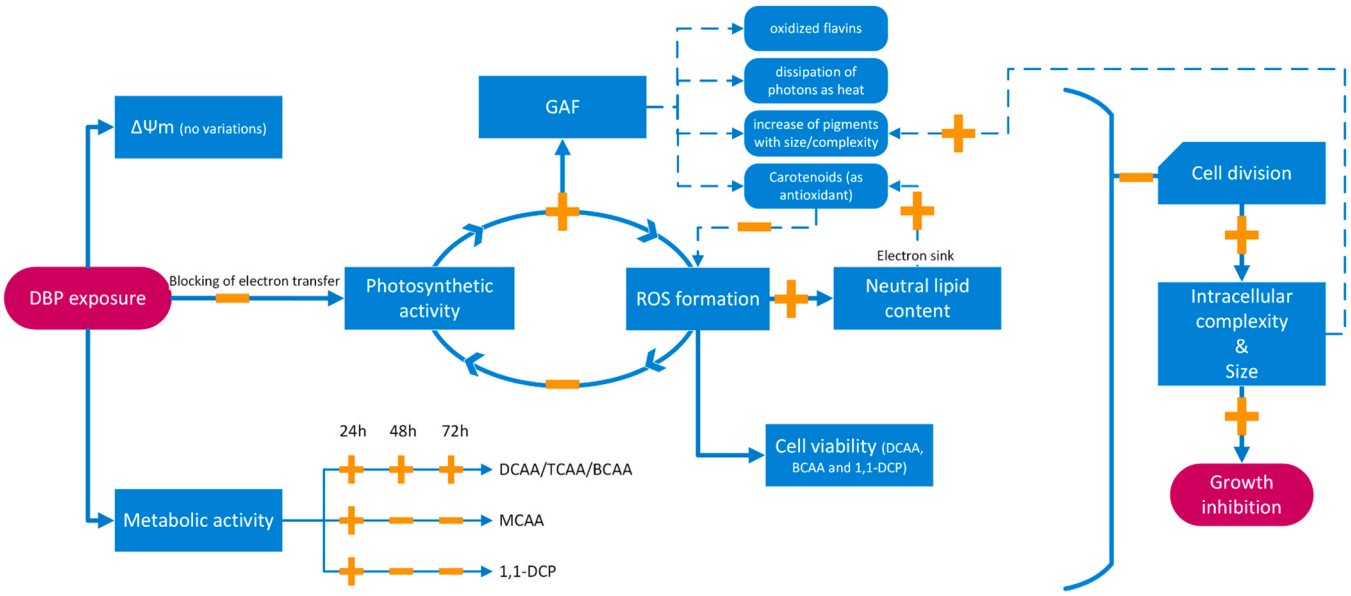

Fig. 7. AOP framework attempt based on the results presented in this work and information available in the literature. It describes the chain of effects occurring in R. subcapitata after the initial exposure to DBPs and leading to growth inhibition (rectangles in red with rounded corners). Sub-lethal parameters measured by FCM are represented in rectangles. Variations are represented by "+ " for an increase and "-" for a decrease. Dashed lines represent potential processes explaining the different observations made. ΔΨm – mitochondrial membrane potential; GAF – green autofluorescence; ROS – reactive oxygen species.

both time steps compared to the first day. In other words, ROS formation tended to decrease with time within specific concentration ranges for BCAA, DCAA and 1,1-DCP. Concerning other conditions of exposure and substances (MCAA and TCAA), non-significant increases in fluorescence intensity were spotted between 48 h and 72 h, mainly at higher concentrations. It was also observed for all DBPs experiments that microalgae with high fluorescence intensity were primarily cells with higher size and intracellular complexity, meaning cells with important oxidative stress were mostly multinucleated (from 59.6% up to 100% of multinucleated cells for all experiments and conditions) (Fig. S6).

3.2.5. *Effects of DBPs on neutral lipid content*

Data related to lipid content are presented in Fig. 5. The cellular parameter neutral lipid content was shown to be sensitive to DBPs. At 24 h, a significant increase in fluorescence intensity was observed for all the DBPs concerning the mid and high range of concentrations tested and remained significant at 48 h and 72 h. However, for all HAAs, content of neutral lipids peaked on the first day of measurements (24 h) and declined significantly for most of the samples at 48 h ($p < 0.05$) before stabilising at 72 h. Similar responses were observed for 1,1-DCP, except for the two highest concentrations where neutral lipid content remained stable at 24 h and 48 h and increased at 72 h ($p < 0.05$). The temporal decreasing trend was recorded for controls on MCAA, TCAA, BCAA and 1,1-DCP experiments but remained less important than for exposed cells. Based on these observations, it is possible to conclude that microalgal cells produce neutral lipids, mainly triacylglycerol (TAGs), in response to the stress and that most of the content is produced early after the exposure as reported in other studies (Hu et al., 2008; Kim et al., 2013; Zienkiewicz et al., 2016).

3.2.6. *Effects of DBPs on esterase activity*

Data related to esterase activity are presented in Fig. 6. Globally, exposure of *R. subcapitata* to DCAA, TCAA and BCAA led to a percentage decrease of metabolically active cells (FDA+) at 48 h and 72 h ($p < 0.05$), a decrease of metabolically inactive cells (FDA-) between 24 h and 48 h ($p < 0.05$) followed by a steady percentage among concentrations at 72 h (2.5–9%), and an increase of metabolically stimulated cells (FDA++) over the entirety of the experiment (FDA++) (up to 74.6% of the cells for BCAA at 72 h for 31.2 $mg.L^{-1}$) (Fig. 6 and Table S3).

Concerning MCAA, a low percentage decrease of metabolically inactive cells (FDA-) was observed at 24 h (from 50.9% to 30.1%) followed by a significant increase at 48 h (from 20.6 up to 54.3%) and 72 h (from 2.7 up to 46.8%) ($p < 0.05$). Moreover, percentage of metabolically active cells (FDA+) decreased at 24 h (from 42.3% to 30.7%), 48 h (from 76.3% to 30.7%) and 72 h (from 94.4% to 34.2%) compared to the control. On the contrary, an increase in metabolically stimulated cells (FDA++) was also spotted, even if most cells were considered inactive at 72 h.

After exposure to 1,1-DCP, percentage of metabolically inactive cells (FDA-) remained steady at all exposure concentrations except 7.2 $mg.L^{-1}$ at 24 h and 1.8 $mg.L^{-1}$ at 48 h (between 41.3% and 77.7%), and was followed by a significant increase at 72 h (from 3.6% for control up to 49.1% for 4.6 $mg.L^{-1}$). Concerning metabolically active cells (FDA+) results showed no differences at 24 h and a significant decrease at 48 h and 72 h. Finally, cells were weakly stimulated at 24 h (FDA++), and at low percentage (between 2.8% and 17.4%) at 48 h and 72 h with no significant changes compared to the control.

4. Discussion

4.1. *Effects of DBPs on physiological and morphological parameters*

All this information can be used attempt to build an AOP describing the chain of effects occurring in algal cells and explain the overall effect of DBPs (Fig. 7).

As already mentioned, *R. subcapitata* exposure to the five DBPs individually led to a decrease red autofluorescence at 72 h, representative of the chlorophyll *a* fluorescence of the microalgae. This can be interpreted as an inhibition of electron flow in the PS II reaction centre at the donor side, which consequently leads to the inhibition of photosynthetic activity as previously seen in Franklin et al. (2001) after exposure to copper. In a previous study, Cui et al. (2021) also observed a significant decrease in photosynthetic activity via the study of chlorophyll *a* fluorescence transient while exposing *Scenedesmus sp.* to MCAA (0.8 and 1.5 $mg.L^{-1}$) at 72 h. The authors concluded that the MoA of MCAA was to block the electron transfer by damaging the thylakoid sheets and disintegrating the pyrenoids inside chloroplasts, inducing a

loss of photosynthetic activity. Chlorophyll *a* fluorescence fluctuations (increase and decrease) were also reported on microalgae for other types of chemicals and linked with effects on the photosynthetic apparatus (Almeida et al., 2021; Franklin et al., 2001; Gebara et al., 2020).

A consequence of photosynthesis inhibition is the potential accumulation of intracellular ROS. Indeed, overproduction and accumulation of intracellular ROS can be a possible consequence of electron transport chain inhibition of the photosystem II (PSII) (Rezayian et al., 2019). Biologically, ROS production in low concentration is a normal process, but when a stress situation occurs an imbalance between production and suppression of ROS occurs leading to damages to cellular components. In our case, the DBPs induced significant ROS formation at 24, 48 and/or 72 h at the highest concentration(s), with amplitudes depending on the specific chemical. This was also demonstrated in the already mentioned Cui et al. (2021) study: the inhibition of the electron transport chain being the initial event leading to the excess of ROS in the case of MCAA exposure towards *Scenedesmus sp.*, which then led to the accumulation of ROS and damage on chloroplasts. In our case, ROS overproduction did not apparently lead to important cellular membrane damage except for 1,1-DCP at 48 h (up to 23% of non-viable cells, with 2% for control), nor on ΔΨm (meaning DBPs did not inhibit ATP synthase) and could be potentially explained by the implementation of antioxidant processes.

In response to ROS accumulation, a shift in lipid production from membrane lipid to neutral lipids storage, mainly as TAGs in the form of lipid droplets can be triggered (Hu et al., 2008; Zhang et al., 2019, 2020). This is often observed in case of oxidative stress resulting from nutrient deprivation, thermal or high light stress (Liu and Benning, 2013; Shi et al., 2017). According to several studies, TAGs are highly reduced molecular species requiring large quantities of NADPH (which are overproduced during oxidative stress) (Shi et al., 2017; Wasylenko et al., 2015) and are capable of decreasing ROS formation therefore allowing the microalgae to continue harvesting light by trapping free electrons (Klok et al., 2013; Morales et al., 2021; Shi et al., 2017). A recent study of Zhang et al. (2019) showed that the specific ROS Hydroxyl radical (OH^-) was mainly responsible for enhancing lipid synthesis in *Chlorella pyrenoidosa* under high light conditions. Neutral lipids may also help maintaining membrane integrity and fluidity. Based on our results, it seems plausible that DBPs exposure induced the formation of ROS, resulting to the observed lipid accumulation early after the exposure, in the form of lipid droplets for carbon and energy storage, but also for their antioxidant properties. Significant decrease observed at 48 h and 72 h could be potentially explained by the cells starting to adapt to their contaminated environment via other detoxification processes.

Another way for the microalgae to cope with ROS accumulation is to synthetize other antioxidant molecules. As we observed in our experiments, green autofluorescence (GAF) increased with the exposure to the five DBPs and this change could be linked to specific intracellular pigments. According to Tang and Dobbs (2007), chlorophylls are not the pigments responsible for GAF, carotenoids could however correspond to this fluorescence wavelength. Usually, carotenoids are complementary pigments to widen the absorption light spectrum of microalgae, but when under stressful conditions, carotenoids are synthesised to protect the cells (Gong and Bassi, 2016; Rammuni et al., 2019). In fact, studies on *Dunaliella salina* and *Chromochloris zofingiensis* concluded that GAF increase that was observed after photo-oxidative stress and nitrogen starvation was caused by the accumulation of secondary carotenoids, such as β-carotene and astaxanthin (Chen et al., 2017; Kleinegris et al., 2010). The first one is β-carotene, which is a carotene with antioxidant properties, emitting at wavelength of 530–570 nm and accumulating in chloroplasts (Chen et al., 2017). The second one, synthetised from β-carotene is the xanthophyll astaxanthin, a potent antioxidant with similar emission wavelength (530–570 nm) produced when the cell is under stressful conditions, and accumulating in lipid droplets (Kawasaki et al., 2020). These two are recognised for their protective capacity against external stresses and are often reported in the literature. According to different sources, they could protect from free radicals, prevent lipid peroxidation, promote functions and stability of the photosynthetic system and membrane integrity (Dieser et al., 2010; Gong and Bassi, 2016; Rammuni et al., 2019; Varela et al., 2015). For example, in *Dunaliella salina*, carotenoids have the ability to deactivate triplet chlorophyll and single oxygen and can accumulate in lipid droplets like TAGs (Kawasaki et al., 2020). Also, biosynthesis and accumulation of these antioxidant molecules have been reported to happen simultaneously with TAG production in algae (Chekanov et al., 2014; Chen et al., 2015; Guo et al., 2021; Ren et al., 2021). Changes in fluorescence observed in the range of 525–50 nm on the flow cytometer could therefore correspond to the production of carotenoids as a protective mechanism against ROS accumulation in the cell. However, another reasonable explanation concerning the increased GAF could be directly linked to the loss of photosynthetic activity. Indeed, a decrease in photochemistry efficiency will lead to the excess accumulation of light energy (photons) which can be dissipated as heat or fluorescence, potentially as GAF (Machado and Soares, 2022). Several studies also show that GAF increase could correspond to intracellular flavins (enzymes involved in redox metabolism) being oxidised due to an increase in ROS content, which would be consistent with the oxidative stress observed in the microalgae (Croce, 2021; Fujita et al., 2005; Lage et al., 2001). Finally, GAF is also correlated with size (R^2 =0.79/0.51/0.55/0.63/0.79 for MCAA/DCAA/TCA/BCAA/1,1-DCP respectively) and intracellular complexity (R^2 =0.9/0.42/0.65/0.6/0.74 for MCAA/DCAA/TCA/BCAA/1,1-DCP respectively). The overall increase observed could therefore simply mean an increase in photosynthetic pigment content, proportionally to the size and complexity of cells (higher pigment content in multinucleated cells).

As mentioned earlier, all samples showed an increase in both size and complexity with the increasing concentration in parallel to GAF, these two morphological parameters seemingly redundant based on the correlation observed after exposure to all substances (Fig. S3). These changes were also observed on *R. subcapitata* and *Chlamydomonas reinhardtii* in the literature and could be explained by the incapacity of the cells to complete their division (Jamers and De Coen, 2010; Mansano et al., 2017; Míguez et al., 2021). Indeed, chemical exposure, while not fully impacting nuclear division, could potentially either delay the cell division cycle or stop it at the last stage before cytokinesis (cytoplasmic division) and lead to accumulation of multinucleated cells (Machado and Soares, 2020). In this form, cells are composed of 2–8 daughter-cell, each with their own organelles, which can explain the higher complexity and size observed (Yamagishi et al., 2017). Switch in lipid production occurring in the cell could be one of the factors leading to cytokinesis inhibition, by making carbon and energy less available for this morphological process (Míguez et al., 2021; Morales et al., 2021). Also, high ROS content observed in these multinucleated cells could partly be explained by the two following hypothesis: (1) the increase in size requires the production of ROS to loosen the cell wall through oxidation cleavage, (2) larger cells have higher chloroplast content and therefore produce more ROS (Ugya et al., 2020).

Concerning metabolic activity, which is monitored by measuring FDA fluorescence intensity, stimulation was observed for all DBPs at 24 h and at 48 h and 72 h for DCAA, TCAA and BCAA. Similar results have been often reported for microalgae concerning various chemicals and could be explained in several ways (Almeida et al., 2021; Jamers et al., 2009; Jamers and De Coen, 2010; Machado and Soares, 2019; Valiente Moro et al., 2012). (1) In response to adverse environmental conditions, metabolic activity could be stimulated due to its involvement in the activation and regulation of detoxification processes, such as the replacement of membrane phospholipids for example (Franklin et al., 2001). (2) An increase in cell membrane permeability due to membrane hyperpolarization could also influence FDA fluorescence intensity, by inducing the uptake of FDA leading to an increase in

fluorescence intensity (Franklin et al., 2001). However, it seems quite unlikely in our case because of the absence or relatively low percentage of non-viable cells observed after exposure to most of the DBPs with propidium iodide. (3) FDA fluorescence intensity could be enhanced by intracellular pH increase (Lage et al., 2001), which was not measured in our study. On the contrary, esterase activity in MCAA and 1,1-DCP experiments was mainly inhibited in the later stage of experiment (at 48 h and 72 h for MCAA and only 72 h for 1,1-DCP) (Fig. 6) which could be explained by either membrane disruption leading to leaking of the dye or simply metabolic inhibition via redox imbalances or alterations in protein synthesis (Seoane et al., 2017a). Still, microalgal cells were partly stimulated after exposure to MCAA at 48 h and 72 h, concerning up to 32% of the population exposed at 26.6 and 45.5 $mg.L^{-1}$. Based on these results, three types of responses could be distinguished: (1) overall stimulation of exposed cells to DCAA, TCAA and BCAA during the entire experiments, (2) stimulation at 24 h followed by inhibition for most of the population with a part of the cells still stimulated at 48 h and 72 h for MCAA and (3) stimulation at 24 h followed by inhibition at 48 h and 72 h for 1,1-DCP.

4.2. Sensitivity of cellular parameters and growth inhibition

After 24 h, the most sensitive cellular parameters were FDA- and FDA+ + for MCAA and TCAA respectively, FDA+ + for DCAA, FDA- for BCAA, and neutral lipid content for 1,1-DCP (Table S3). After 48 h, the most sensitive cellular parameters observed were FDA- and FDA+ for MCAA, FDA+ and FDA+ + for DCAA, FDA+ for TCAA, FDA+ + for BCAA, and GAF for 1,1-DCP (Table S3). After 72 h, the most sensitive cellular parameters were complexity and FDA+ for MCAA, GAF, RAF and FDA+ for DCAA, FDA+ and FDA+ + for TCAA and BCAA respectively, and FDA- and FDA+ for 1,1-DCP (Table S3).

Among the cellular parameter tested, only neutral lipid content showed significant differences at each time step and for each DBP. Nevertheless, metabolic activity, whether low (FDA-), normal (FDA+) or stimulated (FDA++) stood out compared to the other parameters and seemed especially sensitive with HAAs experiments. For 1,1-DCP at 24 h and 48 h, other parameters showed lower LOEC. In our study, the use of FDA seemed relevant to observe physiological disturbances in the case of DBP exposure.

Growth inhibition was found to be less sensitive to DBP exposure than sub-cellular parameters for TCAA and BCAA. For MCAA and DCAA, growth inhibition was found to be as sensitive as the cellular endpoints, but because significative effects were already reported for the first concentrations of exposure (LOEC), no conclusion can be drawn on which parameter is the most sensitive (Table S2 and Table S3). For 1,1-DCP, growth inhibition was more sensitive than sub-cellular endpoints except for cell viability (Fig. 4).

5. Conclusions

In this study, we assessed the sensitivity of several sub-lethal parameters by exposing the freshwater microalgae *Raphidocelis subcapitata* to four haloacetic acids and one haloketone individually. Lipid content, ROS formation, RAF, GAF, size and intracellular complexity were significantly impacted in response to the exposure to the five DBPs. Only mitochondrial membrane potential did not show any variation. Important cellular damages (>10%) were observed only for BCAA and 1,1-DCP and were probably due to ROS formation. The most interesting sub-lethal parameter studied was metabolic activity (esterase activity), for which measurements made over time (24 h, 48 h and 72 h) were shown to be highly relevant. Three types of response were observed depending on the DBP, and high sensitivity except for 1,1-DCP. Further study will be needed to find a mechanistic explanation for these differences observed. An interest should be also given to the natural autofluorescence in microalgae, in particular GAF, for the several biological meaning it could have (notably in antioxidant processes), and the fact that no fluorescent probes are needed to measure it. For that reason, it makes it easy to use and test with other types of stressors. Larger and more complex cells should also be investigated to confirm whether they correspond to multinucleated cells. Data obtained in this study did not allow us to correlate the algal growth inhibition to the chemical structure of the DBPs. Additional experiments would be necessary to check if such correlation could be established between the number of Cl and Br and sub-lethal parameters. Finally, our study demonstrated that the selected cellular parameters were helpful to gain a better understanding of the biological mechanisms leading to growth inhibition on the non-target organism *R. subcapitata*.

CRediT authorship contribution statement

Théo Ciccia: Methodology, Investigation, Formal analysis, Writing - Original Draft. **Pascal Pandard:** Conceptualization, Supervision, Resources, Writing - Review & Editing. **Philippe Ciffroy:** Funding acquisition, Supervision, Writing - Review & Editing. **Nastassia Urien:** Supervision, Writing - Review & Editing. **Léo Lafay:** Supervision, Writing - Review & Editing. **Anne Bado-Nilles:** Conceptualization, Supervision, Resources, Writing - Review & Editing.

Declaration of Competing Interest

The authors declare that they have no known competing financial interests or personal relationships that could have appeared to influence the work reported in this paper.

Data Availability

Data will be made available on request.

Acknowledgments

The authors thank the ANRT (Association Nationale Recherche Technologie) and EDF (Electricité de France) for Théo Ciccia's Ph.D. Grant (convention bourse CIFRE- EDF: No. 3 2020/1386). This study was funded by a partnership between EDF and Ineris.

Appendix A. Supporting information

Supplementary data associated with this article can be found in the online version at doi:10.1016/j.ecoenv.2023.115582.

References

Adan, A., Alizada, G., Kiraz, Y., Baran, Y., Nalbant, A., 2017. Flow cytometry: basic principles and applications. Crit. Rev. Biotechnol. 37, 163–176. https://doi.org/10.3109/07388551.2015.1128876.

Almeida, A.C., Gomes, T., Habuda-Stanić, M., Lomba, J.A.B., Romić, Ž., Turkalj, J.V., Lillicrap, A., 2019. Characterization of multiple biomarker responses using flow cytometry to improve environmental hazard assessment with the green microalgae Raphidocelis subcapitata. Sci. Total Environ. 687, 827–838. https://doi.org/10.1016/j.scitotenv.2019.06.124.

Almeida, A.C., Gomes, T., Lomba, J.A.B., Lillicrap, A., 2021. Specific toxicity of azithromycin to the freshwater microalga Raphidocelis subcapitata. Ecotoxicol. Environ. Saf. 222, 112553. https://doi.org/10.1016/j.ecoenv.2021.112553.

Ankley, G.T., Bennett, R.S., Erickson, R.J., Hoff, D.J., Hornung, M.W., Johnson, R.D., Mount, D.R., Nichols, J.W., Russom, C.L., Schmieder, P.K., Serrrano, J.A., Tietge, J. E., Villeneuve, D.L., 2010. Adverse outcome pathways: a conceptual framework to support ecotoxicology research and risk assessment. Environ. Toxicol. Chem. 29, 730–741. https://doi.org/10.1002/etc.34.

Čertnerová, D., Galbraith, D.W., 2021. Best practices in the flow cytometry of microalgae. Cytom. A, cyto.a.24328. https://doi.org/10.1002/cyto.a.24328.

Ceschin, S., Bellini, A., Scalici, M., 2021. Aquatic plants and ecotoxicological assessment in freshwater ecosystems: a review. Environ. Sci. Pollut. Res. 28, 4975–4988. https://doi.org/10.1007/s11356-020-11496-3.

Chae, Y., Kim, D., An, Y.-J., 2016. Effect of fluoride on the cell viability, cell organelle potential, and photosynthetic capacity of freshwater and soil algae. Environ. Pollut. 219, 359–367. https://doi.org/10.1016/j.envpol.2016.10.063.

Charles, S., Veber, P., Delignette-Muller, M.L., 2018. MOSAIC: a web-interface for statistical analyses in ecotoxicology. Environ. Sci. Pollut. Res. 25, 11295–11302. https://doi.org/10.1007/s11356-017-9809-4.

Chekanov, K., Lobakova, E., Selyakh, I., Semenova, L., Sidorov, R., Solovchenko, A., 2014. Accumulation of astaxanthin by a new haematococcus pluvialis strain BM1 from the White Sea Coastal Rocks (Russia). Mar. Drugs 12, 4504–4520. https://doi.org/10.3390/md12084504.

Cheloni, G., Slaveykova, V., 2018. Photo-oxidative stress in green algae and cyanobacteria. React. Oxyg. Species. https://doi.org/10.20455/ros.2018.819.

Chen, G., Wang, B., Han, D., Sommerfeld, M., Lu, Y., Chen, F., Hu, Q., 2015. Molecular mechanisms of the coordination between astaxanthin and fatty acid biosynthesis in *Haematococcus pluvialis* (Chlorophyceae). Plant J. 81, 95–107. https://doi.org/10.1111/tpj.12713.

Chen, J., Wei, D., Pohnert, G., 2017. Rapid estimation of astaxanthin and the carotenoid-to-chlorophyll ratio in the green microalga chromochloris zofingiensis using flow cytometry. Mar. Drugs 15, 231. https://doi.org/10.3390/md15070231.

Ciffroy, P., Urien, N., 2021. A probabilistic model for assessing uncertainty and sensitivity in the prediction of monochloramine loss in French river waters. Water Res 202, 117383. https://doi.org/10.1016/j.watres.2021.117383.

Coniglio, M.A., Strano, V., D'Angelo, S., Guercio, M.A., Spada, R., Melada, S., 2015. Effectiveness of in-situ generated monochloramine for the control of legionella in a real industrial cooling tower. Glob. J. Med. Res. 15, 9–15.

Cowman, G.A., Singer, P.C., 1996. Effect of bromide ion on haloacetic acid speciation resulting from chlorination and chloramination of aquatic humic substances. Environ. Sci. Technol. 30, 16–24. https://doi.org/10.1021/es9406905.

Croce, A.C., 2021. Light and autofluorescence, multitasking features in living organisms. Photochem 1, 67–125. https://doi.org/10.3390/photochem1020007.

Cui, H., Chen, B., Jiang, Y., Tao, Y., Zhu, X., Cai, Z., 2021. Toxicity of 17 disinfection by-products to different trophic levels of aquatic organisms: ecological risks and mechanisms. Environ. Sci. Technol., acs.est.0c08796 https://doi.org/10.1021/acs.est.0c08796.

Cui, H., Zhu, X., Zhu, Y., Huang, Y., Chen, B., 2022. Ecotoxicological effects of DBPs on freshwater phytoplankton communities in co-culture systems. J. Hazard. Mater. 421, 126679. https://doi.org/10.1016/j.jhazmat.2021.126679.

Diehl, A.C., Speitel, G.E., Symons, J.M., Krasner, S.W., Hwang, C.J., Barrett, S.E., 2000. DBP formation during chloramination. J. - Am. Water Works Assoc. 92, 76–90. https://doi.org/10.1002/j.1551-8833.2000.tb08961.x.

Dieser, M., Greenwood, M., Foreman, C.M., 2010. Carotenoid pigmentation in antarctic heterotrophic bacteria as a strategy to withstand environmental stresses. Arct. Antarct. Alp. Res. 42, 396–405. https://doi.org/10.1657/1938-4246-42.4.396.

Dong, H., Zhang, H., Wang, Y., Qiang, Z., Yang, M., 2021. Disinfection by-product (DBP) research in China: are we on the track? J. Environ. Sci., S1001074221001108 https://doi.org/10.1016/j.jes.2021.03.023.

Duirk, S.E., Gombert, B., Choi, J., L. Valentine, R., 2002. Monochloramine loss in the presence of humic acid. J. Environ. Monit. 4, 85–89. https://doi.org/10.1039/B106047N.

Duirk, S.E., Gombert, B., Croué, J.-P., Valentine, R.L., 2005. Modeling monochloramine loss in the presence of natural organic matter. Water Res 39, 3418–3431. https://doi.org/10.1016/j.watres.2005.06.003.

Dupraz, V., Ménard, D., Akcha, F., Budzinski, H., Stachowski-Haberkorn, S., 2019. Toxicity of binary mixtures of pesticides to the marine microalgae Tisochrysis lutea and Skeletonema marinoi: substance interactions and physiological impacts. Aquat. Toxicol. 211, 148–162. https://doi.org/10.1016/j.aquatox.2019.03.015.

Dupuy, M., Mazoua, S., Berne, F., Bodet, C., Garrec, N., Herbelin, P., Ménard-Szczebara, F., Oberti, S., Rodier, M.-H., Soreau, S., Wallet, F., Héchard, Y., 2011. Efficiency of water disinfectants against Legionella pneumophila and Acanthamoeba. Water Res 45, 1087–1094. https://doi.org/10.1016/j.watres.2010.10.025.

Faust, M., Altenburger, R., Backhaus, T., Blanck, H., Boedeker, W., Gramatica, P., Hamer, V., Scholze, M., Vighi, M., Grimme, L.H., 2003. Joint algal toxicity of 16 dissimilarly acting chemicals is predictable by the concept of independent action. Aquat. Toxicol. 63, 43–63. https://doi.org/10.1016/S0166-445X(02)00133-9.

Fisher, D., Yonkos, L., Ziegler, G., Friedel, E., Burton, D., 2014. Acute and chronic toxicity of selected disinfection byproducts to Daphnia magna, Cyprinodon variegatus, and Isochrysis galbana. Water Res 55, 233–244. https://doi.org/10.1016/j.watres.2014.01.056.

Franklin, N.M., Stauber, J.L., Lim, R.P., 2001. Development of flow cytometry-based algal bioassays for assessing toxicity of copper in natural waters. Environ. Toxicol. Chem. 20, 160–170. https://doi.org/10.1002/etc.5620200118.

Fujita, S., Iseki, M., Yoshikawa, S., Makino, Y., Watanabe, M., Motomura, T., Kawai, H., Murakami, A., 2005. Identification and characterization of a fluorescent flagellar protein from the brown alga *Scytosiphon lomentaria* (Scytosiphonales, Phaeophyceae): a flavoprotein homologous to Old Yellow Enzyme. Eur. J. Phycol. 40, 159–167. https://doi.org/10.1080/09670260500063193.

Gebara, R.C., Alho, L. de O.G., Rocha, G.S., Mansano, A. da S., Melão, M. da G.G., 2020. Zinc and aluminum mixtures have synergic effects to the algae Raphidocelis subcapitata at environmental concentrations. Chemosphere 242, 125231. https://doi.org/10.1016/j.chemosphere.2019.125231.

Gong, M., Bassi, A., 2016. Carotenoids from microalgae: a review of recent developments. Biotechnol. Adv. 34, 1396–1412. https://doi.org/10.1016/j.biotechadv.2016.10.005.

Guo, H., Li, T., Zhao, Y., Yu, X., 2021. Role of copper in the enhancement of astaxanthin and lipid coaccumulation in Haematococcus pluvialis exposed to abiotic stress conditions. Bioresour. Technol. 335, 125265. https://doi.org/10.1016/j.biortech.2021.125265.

Hanigan, D., Truong, L., Simonich, M., Tanguay, R., Westerhoff, P., 2017. Zebrafish embryo toxicity of 15 chlorinated, brominated, and iodinated disinfection by-products. J. Environ. Sci., Water Treat. Disinfect. -Prod. 58, 302–310. https://doi.org/10.1016/j.jes.2017.05.008.

Hu, Q., Sommerfeld, M., Jarvis, E., Ghirardi, M., Posewitz, M., Seibert, M., Darzins, A., 2008. Microalgal triacylglycerols as feedstocks for biofuel production: perspectives and advances. Plant J. 54, 621–639. https://doi.org/10.1111/j.1365-313X.2008.03492.x.

Jamers, A., De Coen, W., 2010. Effect assessment of the herbicide paraquat on a green alga using differential gene expression and biochemical biomarkers. Environ. Toxicol. Chem. 29, 893–901. https://doi.org/10.1002/etc.102.

Jamers, A., Lenjou, M., Deraedt, P., Bockstaele, D.V., Blust, R., Coen, W. de, 2009. Flow cytometric analysis of the cadmium-exposed green alga Chlamydomonas reinhardtii (Chlorophyceae). Eur. J. Phycol. 44, 541–550. https://doi.org/10.1080/09670260903118214.

Kawasaki, S., Yamazaki, K., Nishikata, T., Ishige, T., Toyoshima, H., Miyata, A., 2020. Photooxidative stress-inducible orange and pink water-soluble astaxanthin-binding proteins in eukaryotic microalga. Commun. Biol. 3, 490. https://doi.org/10.1038/s42003-020-01206-7.

Kim, S., Kim, H., Ko, D., Yamaoka, Y., Otsuru, M., Kawai-Yamada, M., Ishikawa, T., Oh, H.-M., Nishida, I., Li-Beisson, Y., Lee, Y., 2013. Rapid induction of lipid droplets in chlamydomonas reinhardtii and chlorella vulgaris by brefeldin A. PLoS ONE 8, e81978. https://doi.org/10.1371/journal.pone.0081978.

Kleinegris, D.M.M., van Es, M.A., Janssen, M., Brandenburg, W.A., Wijffels, R.H., 2010. Carotenoid fluorescence in Dunaliella salina. J. Appl. Phycol. 22, 645–649. https://doi.org/10.1007/s10811-010-9505-y.

Klok, A.J., Martens, D.E., Wijffels, R.H., Lamers, P.P., 2013. Simultaneous growth and neutral lipid accumulation in microalgae. Bioresour. Technol. 134, 233–243. https://doi.org/10.1016/j.biortech.2013.02.006.

Lage, O.M., Sansonetty, F., O'Connor, J.-E., Parente, A.M., 2001. Flow cytometric analysis of chronic and acute toxicity of copper(II) on the marine dinoflagellateAmphidinium carterae. Cytometry 44, 226–235 https://doi.org/10.1002/1097-0320(20010701)44:3<226::AID-CYTO1115>3.0.CO;2-9.

Lewis, M.A., 1990. Are laboratory-derived toxicity data for freshwater algae worth the effort? Environ. Toxicol. Chem. 9, 1279–1284. https://doi.org/10.1002/etc.5620091006.

Liu, B., Benning, C., 2013. Lipid metabolism in microalgae distinguishes itself. Curr. Opin. Biotechnol. 24, 300–309. https://doi.org/10.1016/j.copbio.2012.08.008.

Liu, W., Chen, S., Quan, X., Jin, Y.-H., 2008. Toxic effect of serial perfluorosulfonic and perfluorocarboxylic acids on the membrane system of a freshwater alga measured by flow cytometry. Environ. Toxicol. Chem. 27, 1597–1604. https://doi.org/10.1897/07-459.1.

Machado, M.D., Soares, E.V., 2015. Use of a fluorescence-based approach to assess short-term responses of the alga Pseudokirchneriella subcapitata to metal stress. J. Appl. Phycol. 27, 805–813. https://doi.org/10.1007/s10811-014-0351-1.

Machado, M.D., Soares, E.V., 2019. Impact of erythromycin on a non-target organism: cellular effects on the freshwater microalga Pseudokirchneriella subcapitata. Aquat. Toxicol. 208, 179–186. https://doi.org/10.1016/j.aquatox.2019.01.014.

Machado, M.D., Soares, E.V., 2020. Reproductive cycle progression arrest and modification of cell morphology (shape and biovolume) in the alga Pseudokirchneriella subcapitata exposed to metolachlor. Aquat. Toxicol. 222, 105449. https://doi.org/10.1016/j.aquatox.2020.105449.

Machado, M.D., Soares, E.V., 2021. Exposure of the alga Pseudokirchneriella subcapitata to environmentally relevant concentrations of the herbicide metolachlor: impact on the redox homeostasis. Ecotoxicol. Environ. Saf. 207, 111264. https://doi.org/10.1016/j.ecoenv.2020.111264.

Machado, M.D., Soares, E.V., 2022. Life and death of pseudokirchneriella subcapitata: physiological changes during chronological aging. Appl. Microbiol. Biotechnol. 106, 8245–8258. https://doi.org/10.1007/s00253-022-12267-5.

Machado, M.D., Lopes, A.R., Soares, E.V., 2015. Responses of the alga Pseudokirchneriella subcapitata to long-term exposure to metal stress. J. Hazard. Mater. 296, 82–92. https://doi.org/10.1016/j.jhazmat.2015.04.022.

Mansano, A.S., Moreira, R.A., Dornfeld, H.C., Freitas, E.C., Vieira, E.M., Sarmento, H., Rocha, O., Seleghim, M.H.R., 2017. Effects of diuron and carbofuran and their mixtures on the microalgae Raphidocelis subcapitata. Ecotoxicol. Environ. Saf. 142, 312–321. https://doi.org/10.1016/j.ecoenv.2017.04.024.

Míguez, L., Esperanza, M., Seoane, M., Cid, Á., 2021. Assessment of cytotoxicity biomarkers on the microalga Chlamydomonas reinhardtii exposed to emerging and priority pollutants. Ecotoxicol. Environ. Saf. 208, 111646. https://doi.org/10.1016/j.ecoenv.2020.111646.

Morales, M., Aflalo, C., Bernard, O., 2021. Microalgal lipids: a review of lipids potential and quantification for 95 phytoplankton species. Biomass-.-. Bioenergy 150, 106108. https://doi.org/10.1016/j.biombioe.2021.106108.

Nyholm, N., Källqvist, T., 1989. Methods for growth inhibition toxicity tests with freshwater algae. Environ. Toxicol. Chem. 8, 689–703. https://doi.org/10.1002/etc.5620080807.

OECD, 2011. Test No. 201: Alga, Growth Inhibition Test, OECD Guidelines for the Testing of Chemicals, Section 2: Effects on Biotic Systems. OECD Publishing. https://doi.org/10.1787/9789264069923-en.

Rammuni, M.N., Ariyadasa, T.U., Nimarshana, P.H.V., Attalage, R.A., 2019. Comparative assessment on the extraction of carotenoids from microalgal sources: Astaxanthin from H. pluvialis and β-carotene from D. salina. Food Chem. 277, 128–134. https://doi.org/10.1016/j.foodchem.2018.10.066.

Ren, Y., Sun, H., Deng, J., Huang, J., Chen, F., 2021. Carotenoid production from microalgae: biosynthesis, salinity responses and novel biotechnologies. Mar. Drugs 19, 713. https://doi.org/10.3390/md19120713.

Reynolds, C.S., 1984. The ecology of freshwater phytoplankton, Cambridge studies in ecology. Cambridge University Press, Cambridge; New York.
Rezayian, M., Niknam, V., Ebrahimzadeh, H., 2019. Oxidative damage and antioxidative system in algae. Toxicol. Rep. 6, 1309–1313. https://doi.org/10.1016/j.toxrep.2019.10.001.
Richardson, S.D., Postigo, C., 2011. Drinking Water Disinfection By-products. In: Barceló, D. (Ed.), Emerging Organic Contaminants and Human Health, The Handbook of Environmental Chemistry. Springer Berlin Heidelberg, Berlin, Heidelberg, pp. 93–137. https://doi.org/10.1007/698_2011_125.
Roberts, J.F., van Egmond, R., Price, O.R., 2010. Toxicity of haloacetic acids to freshwater algae. Ecotoxicol. Environ. Saf. 73, 56–61. https://doi.org/10.1016/j.ecoenv.2009.09.013.
Rojíčková, R., Maršálek, B., 1999. Selection and sensitivity comparisons of algal species for toxicity testing. Chemosphere 38, 3329–3338. https://doi.org/10.1016/S0045-6535(98)00566-9.
Seoane, M., Esperanza, M., Cid, Á., 2017a. Cytotoxic effects of the proton pump inhibitor omeprazole on the non-target marine microalga Tetraselmis suecica. Aquat. Toxicol. 191, 62–72. https://doi.org/10.1016/j.aquatox.2017.08.001.
Seoane, M., Esperanza, M., Rioboo, C., Herrero, C., Cid, Á., 2017b. Flow cytometric assay to assess short-term effects of personal care products on the marine microalga Tetraselmis suecica. Chemosphere 171, 339–347. https://doi.org/10.1016/j.chemosphere.2016.12.097.
Shi, K., Gao, Z., Shi, T.-Q., Song, P., Ren, L.-J., Huang, H., Ji, X., 2017. Reactive oxygen species-mediated cellular stress response and lipid accumulation in oleaginous microorganisms: the state of the art and future perspectives. Front. Microbiol. 8, 793. https://doi.org/10.3389/fmicb.2017.00793.
Silva, A., Figueiredo, S.A., Sales, M.G., Delerue-Matos, C., 2009. Ecotoxicity tests using the green algae Chlorella vulgaris—a useful tool in hazardous effluents management. J. Hazard. Mater. 167, 179–185. https://doi.org/10.1016/j.jhazmat.2008.12.102.
Steadman Tyler, C.R., Sanders, C.K., Erickson, R.S., Dale, T., Twary, S.N., Marrone, B.L., 2019. Functional and phenotypic flow cytometry characterization of Picochlorum soloecismus. Algal Res 43, 101614. https://doi.org/10.1016/j.algal.2019.101614.
Tang, Y.Z., Dobbs, F.C., 2007. Green autofluorescence in dinoflagellates, diatoms, and other microalgae and its implications for vital staining and morphological studies. Appl. Environ. Microbiol. 73, 2306–2313. https://doi.org/10.1128/AEM.01741-06.
Ugya, A.Y., Imam, T.S., Li, A., Ma, J., Hua, X., 2020. Antioxidant response mechanism of freshwater microalgae species to reactive oxygen species production: a mini review. Chem. Ecol. 36, 174–193. https://doi.org/10.1080/02757540.2019.1688308.
Valiente Moro, C., Bricheux, G., Portelli, C., Bohatier, J., 2012. Comparative effects of the herbicides chlortoluron and mesotrione on freshwater microalgae. Environ. Toxicol. Chem. 31, 778–786. https://doi.org/10.1002/etc.1749.
Varela, J.C., Pereira, H., Vila, M., León, R., 2015. Production of carotenoids by microalgae: achievements and challenges. Photosynth. Res. 125, 423–436. https://doi.org/10.1007/s11120-015-0149-2.
Vikesland, P., 2001. Monochloramine decay in model and distribution system waters. Water Res 35, 1766–1776. https://doi.org/10.1016/S0043-1354(00)00406-1.
Wasylenko, T.M., Ahn, W.S., Stephanopoulos, G., 2015. The oxidative pentose phosphate pathway is the primary source of NADPH for lipid overproduction from glucose in Yarrowia lipolytica. Metab. Eng. 30, 27–39. https://doi.org/10.1016/j.ymben.2015.02.007.
Yamagishi, T., Yamaguchi, H., Suzuki, S., Horie, Y., Tatarazako, N., 2017. Cell reproductive patterns in the green alga Pseudokirchneriella subcapitata (=Selenastrum capricornutum) and their variations under exposure to the typical toxicants potassium dichromate and 3,5-DCP. PLOS ONE 12, e0171259. https://doi.org/10.1371/journal.pone.0171259.
Zhang, L., Liao, C., Yang, Y., Wang, Y.-Z., Ding, K., Huo, D., Hou, C., 2019. Response of lipid biosynthesis in Chlorella pyrenoidosa to intracellular reactive oxygen species level under stress conditions. Bioresour. Technol. 287, 121414. https://doi.org/10.1016/j.biortech.2019.121414.
Zhang, S., He, Y., Sen, B., Wang, G., 2020. Reactive oxygen species and their applications toward enhanced lipid accumulation in oleaginous microorganisms. Bioresour. Technol. 307, 123234. https://doi.org/10.1016/j.biortech.2020.123234.
Zienkiewicz, K., Du, Z.-Y., Ma, W., Vollheyde, K., Benning, C., 2016. Stress-induced neutral lipid biosynthesis in microalgae — molecular, cellular and physiological insights. Biochim. Biophys. Acta BBA - Mol. Cell Biol. Lipids 1861, 1269–1281. https://doi.org/10.1016/j.bbalip.2016.02.008.